J Mater Sci (2009) 44:1287–1293
DOI 10.1007/s10853-009-3277-2

Nanostructured physical gel of SBS block copolymer and Ag/DT/SBS nanocomposites

Laura Peponi · Agnieszka Tercjak · Luigi Torre · Iñaki Mondragon · Josè M. Kenny

Received: 15 December 2008 / Accepted: 14 January 2009 / Published online: 7 February 2009

Abstract Thermoreversible physical gels of poly(styrene-*b*-butadiene-*b*-styrene) (SBS), formed by the dissolution of the block copolymer in a mid-block-selective solvent (THF), have been studied and characterized with particular attention to their morphology and rheological behavior. The effects of the addition of silver (Ag) nanoparticles to the SBS matrix, on the behavior of the physical gels, were also studied. The external surface of the Ag nanoparticles has been modified by using as surfactant material, dodecanethiol, in order to achieve their confinement in just one block of the SBS block copolymer matrix. The results of this study show that the gel stability is not affected by the presence of Ag nanoparticles. In fact, the micellar domains of the nanocomposite gel based on SBS block copolymer and Ag nanoparticles has been obtained and the physical gel behavior have been confirmed by rheological analysis.

Introduction

Block copolymers (BC) are a class of materials that have been extensively studied in recent years as versatile systems for engineering nanotechnologies because of their ability to self-assemble in nano-ordered structures [1–4]. The self-assembly processes in copolymers are a consequence of the microphase separation between the dissimilar chains covalently linked together. The equilibrium morphology of diblock copolymers is obtained after segregation into lamellae, gyroid, cylinders, or spheres arranged on a body-center cubic or hexagonal packed lattice [5–9]. Concerning the rheological behavior, the low-frequency dynamical viscoelastic response of BC gives information about the miscibility or immiscibility of the components being sensitive to the change in their structure and morphology [10–12].

When exposed to a block selective solvent, BC can form reversible physical gels [13–15]. This unique behavior results from the formation of a three-dimensional network of physically crosslinked flexible polymer chains. This physical connection takes advantage of the ability of BC to form elastic solids via self-assembly, with mid-blocks bridging aggregated end-block micelles [16–22]. The interaction between micelles depends on the temperature, the solvent activity, and on the architecture of the block copolymer. For example, it is well known that AB diblock copolymers formed by two incompatible polymer blocks aggregate into micelles when mixed with a solvent that dissolves one of the blocks and precipitates the second one [13]. The resulting microdomains consist of a dense core of A-blocks surrounded by a corona of B-block chains extending into the matrix of B-selective solvent. Microdomains can have spherical, rod, or disk shape.

Although two diblock micelles in a good solvent always repel each other, the bridging of triblock chains between micelles generates an entropic attraction [13, 23–28]. The dynamics of bridging plays here an important role. In fact, as opposed to monomer–monomer attraction in poor solvents, bridging interactions are not instantaneous. Since the bridging is an activation process, long-lived, metastable configurations which are free of bridging are possible. The theory of bridging interactions, which leads to the formation of physical mesogels, has been extensively studied [29–32].

L. Peponi · L. Torre · J. M. Kenny (✉)
Materials Engineering Centre, University of Perugia, Loc. Pentima Bassa, 21, 05100 Terni, Italy
e-mail: jkenny@unipg.it

L. Peponi · A. Tercjak · I. Mondragon
'Materials + Technologies' Group, Departmento Ingeniería Química y M. Ambiente, Escuela Politécnica, Universidad País Vasco/Euskal Herriko Unibertsitatea, Pza. Europa 1, 20018 Donostia-San Sebastián, Spain

A similar behavior is expected in ABA symmetric triblock polymer systems. When ABA copolymers are dissolved in a mid-block selective solvent, they form gels that retain many desirable properties of the liquid phase while adding the ease of handling and robust nature of an elastic solid [13]. Additionally, the thermoreversible nature of the gel transition makes these systems ideal from a processing perspective [18]. They have been used, for example, in ceramics [18, 19], model pressure-sensitive adhesives [20, 21], and for hydrogels in tissue engineering [25].

Thermoreversibility of triblock gels originates from the temperature dependency of the interaction parameter between the end-blocks and the solvent. Systems with long-range ordering of micelles can be characterized by two transition temperatures. The first one is the critical micelle temperature (CMT) at which the end-block aggregates, commonly referred as micelles, are formed. The second one is the glass transition temperature (T_g) of the slightly swollen end-block domains [13]. In case of triblock copolymers, however, the polymer mid-blocks at the core of the microdomains form either loops or bridges, depending on whether the copolymer end-blocks are located in the same or in different domains. These features are reminiscent of biopolymers and, in particular, proteins. These qualitatively novel effects are thus of inherent interest within the framework of both polymer science and the biophysics of biopolymers.

Our discussion is confined to the morphological and rheological analysis of the physical gel obtained from a solution of poly(styrene-*b*-butadiene-*b*-styrene) (SBS) in tetrahydrofuran (THF). Moreover, a preliminary study of surfactant-coated Ag nanoparticles/SBS nanocomposite gel is also reported in terms of its morphological and rheological properties. The use of triblock copolymers provides more flexibility in controlling the gel structure and physical properties through block length, block composition, triblock copolymer concentration, and the choice of monomer units [10]. In the research reported here, the morphologies of these materials were analyzed and compared using atomic force microscopy (AFM), and their viscoelastic behavior were studied by dynamic mechanical characterization at low frequencies. The rheological characterization of these gels in the range of small deformations is relevant for many industrial applications [13, 25–31].

Experimental section

Materials

A commercial poly(styrene-*b*-butadyene-*b*-styrene) block copolymer Kraton SBS D-1101 with 31% of styrene, kindly supplied by Kraton Polymer®, was used in this work. The molecular weight and the polydispersion index of the BC were determined by gel permeation chromatography (GPC). Tetrahydrofuran (THF) from Sigma Aldrich was used as solvent. Silver (Ag) nanoparticles P203 were supplied by Cima Nano Tech®. They had a specific surface area of 4.9 m^2/g and a particle size distribution varying from 20 to 70 nm. To incorporate metallic nanoparticles in the polymeric matrix, dodecanethiol (DT) was used as surfactant.

Sample preparation

THF is known to be a butadiene selective solvent, as can be shown considering its solubility parameter which is very close to that calculated using the Hoftyzer and Van Krevelen theory [33], and reported for butadiene in Table 1. Therefore, pellets of the copolymer were dissolved in THF and stirred for 12 h to obtain physical gels (PG-SBS) with different concentrations (2, 3, 5, 7 and 10 wt%).

The formation of the gel required several days when the solution was left at room conditions. Nanocomposite gels (PG-Ag/SBS) were obtained by dissolving the SBS triblock copolymer in the suspension of DT-Ag nanoparticles in THF, previously prepared by sonication, using a microprocessor sonicator 750 W, Vibracell 75043 from Bioblock Scientific with amplitude of 25%. Sonication was necessary because of the very high surface energy of Ag [34].

Morphological analysis

The morphologies of the SBS physical gels (obtained with 3 wt% of SBS in THF cast on a mica support) and of their nanocomposite gels were investigated using atomic force microscopy (AFM). AFM images were obtained in tapping mode (TM) with a scanning probe microscope (Nanoscope IIIa, Multimode™ from Digital Instruments), equipped with an integrated silicon tip/cantilever having a resonance frequency ~300 kHz. The height and phase images were obtained under ambient conditions with typical scan rates of 0.5–1 line/s, using a scan head with a maximum range of 16 × 16 μm.

Physico-chemical analysis

Gel permeation chromatography was performed using Perkin-Elmer LC-235 equipment with a UV detector set at

Table 1 Main characteristics for the SBS block copolymer analyzed

Material	PS (wt%)	M_w (g/mol)	PD	δ	
				PS	PB
SBS D1101	31	150,000	1.8	19.08	17.05

M_w molecular weight, *PD* polydispersity index, δ solubility parameter

245 nm and a refractive index detector LC-30 RI. The mobile phase was THF at a flow rate of 1 mL/min. Number and average molecular weights were calculated using a universal calibration method with polystyrene standards. Perkin-Elmer UV/VISNIR, mod. 135, was used to confirm the transparency of the gels obtained in this work, and the UV–Vis spectroscopy was performed by scanning the samples between 250 and 1200 nm.

Rheological tests

A parallel plates rheometer, Advanced Rheometrics Expansion System, Ares, with plates of 25 mm diameter was used; the gap between the plates was around 1 mm. Three types of experiments were performed: dynamic temperature ramps, dynamic strain sweeps, and dynamic frequency sweeps. Dynamic strain sweep tests at a constant frequency were used to locate the linear viscoelastic (LVE) region in which G' and G'' were independent on the strain amplitude. Rheological experiments on the physical gels were conducted by casting the gel in the parallel plates at room temperature. Isothermal frequency sweeps at 30 °C over an angular frequency (ω) ranging from 0.05 to 100 s^{-1} were performed at a constant stress chosen such that the resulting strain was in LVE region. Linearity was found for the gelling sample when the strain amplitude was 1%. At the end of isochronal dynamic temperature ramp, tests were performed from 30 to 120°C at a heating rate of 5 °C min^{-1} and at a frequency of 6.28 rad s^{-1}. The temperature dependence of the dynamic moduli was measured on heating and cooling at a strain of 1% and a rate of 5 °C min^{-1}. Taking the sensibility of the rheometer into account, the error of the value of the storage and loss moduli in each data point was ±5%. The transducer operating range was set to 0.2–200 g cm or 0.2–2000 g cm depending on the measured torque values. Data were collected and analyzed using Advanced Rheometric Expansion System software.

Results and discussion

SBS gels obtained by dissolution of different concentrations of the block copolymer (3, 5, 7, and 10 wt%) in THF were analyzed. To confirm their transparent behavior, UV–Vis spectra are reported in Fig. 1. The absorbance values very close to zero for the different PG-SBS confirm the transparency of these gels in the visible light range. In Fig. 1, the spectrum of the PG-Ag/SBS is also reported, showing that the nanocomposite gel is also transparent in the visible light range. The rheological analysis for both chemical (covalent cross-linked) and physical (reversible association) gels is very important to investigate their viscoelastic behavior. The liquid-like or solid-like behavior of a material can be determined by analyzing the dynamic moduli at low frequency. The typical rheological behavior of a viscous fluid, such as a polymer solution or melt, is characterized by a dynamic storage modulus G' smaller than the loss modulus and by a dependency of both moduli on the angular frequency (ω) in the low-frequency region: $G' \sim \omega^2$ and $G'' \sim \omega$. On the other hand, the solid-like behavior is characterized by a storage modulus significantly larger than the loss modulus and frequency independent at low frequencies.

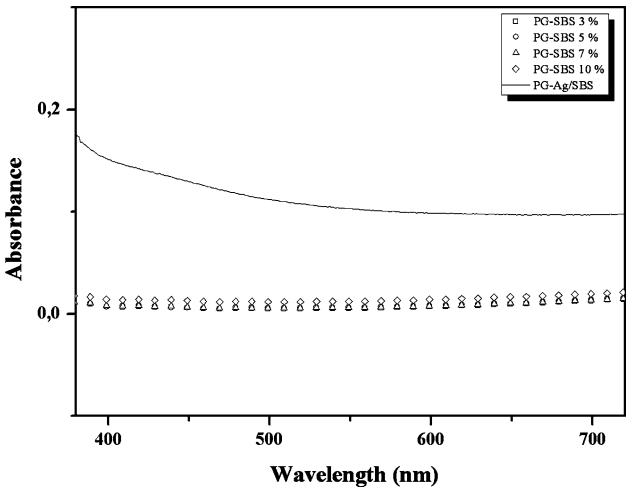

Fig. 1 UV–Vis spectra obtained in the visible range for the SBS gels obtained for different TFH concentrations: 3, 5, 7 and 10 wt%, and for the gelled nanocomposite

The rheological behavior in terms of storage modulus (filled square), loss modulus (unfilled square) of the PG-SBS at 3 wt% is reported in Fig. 2. It is worth to note that G' values are much higher than G'' throughout the entire range of investigated frequencies; thus, indicating that the

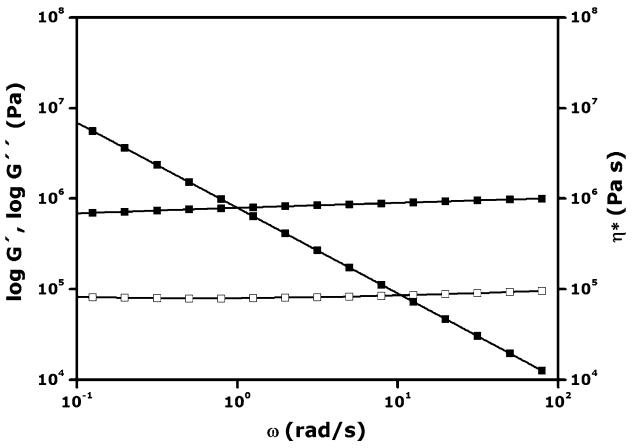

Fig. 2 Frequency dependence of storage (*filled square*) and loss (*unfilled square*) moduli and complex viscosity η^* (*filled square*) for PG-SBS at 30 °C

sample gel presents a typical solid-like behavior. However, the complex viscosity does not reach a plateau value in the entire range of frequencies.

The viscoelastic nature of the physical gel obtained is confirmed by the plots of Fig. 3, where the values of log of G' and G'' are reported as a function of the frequency at different temperatures, the set of curve obtained is typical of superimposible viscoelastic curves.

The rheological analysis of PG-SBS samples has confirmed the thermoreversible physical gel behavior. In fact, as shown in Fig. 4, PG-SBS looses its solid-like behavior when heated above 80 °C. Moreover, the results reported in Fig. 4 show that the reversibility of the gels was preserved when thermal cycles were applied in the interval (40–120 °C). Indeed, the gelling behavior of the sample was maintained up to the fifth heating ramp. In fact, the shape of viscoelastic relaxation spectrum shifts to higher storage modulus values with increasing the number of heating/cooling cycles, thus indicating a slight hardening of the material, up to the fifth cycle, which could correspond to the beginning of the loss of the gelling ability of the SBS block copolymer.

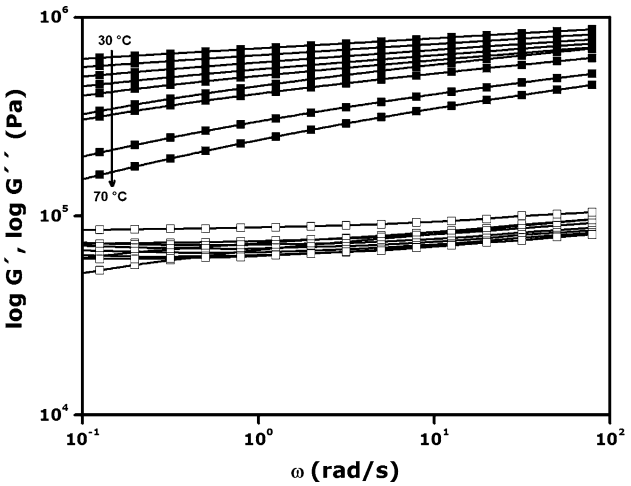

Fig. 3 Frequency dependence of storage (*filled square*) and loss (*unfilled square*) moduli for PG-SBS repeated at different temperature from 30 to 70 °C

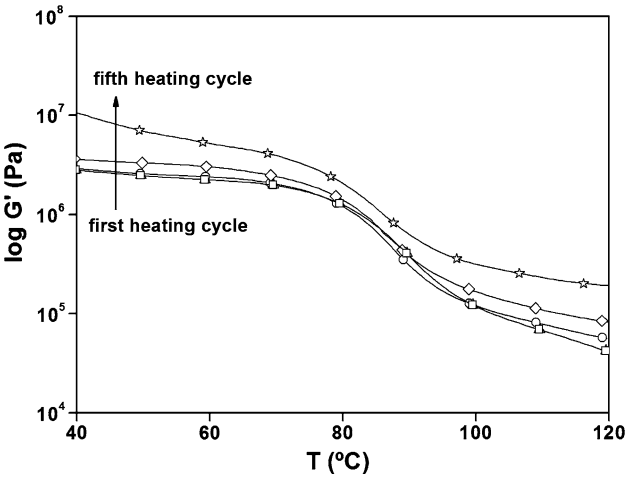

Fig. 4 Isochronal temperature ramps ($\gamma = 1\%$, $\omega = 1$ Hz, heating/cooling rate = 5 °C/min) from 40 to 120 °C for PG-SBS. Comparison in terms of G' for five heating/cooling cycles (for clarity, only the heating cycles are reported)

Figure 5 reports the viscoelastic behavior of the same SBS physical gel reported in Fig. 4 during the fifth heating/cooling cycle test. The hysteresis behavior of the gelling sample is still detectable after five cycles. It is worth to note that even in the fifth heating/cooling cycle, gelation, indicated by the plateau in G', is clearly evident. Another important aspect is that, the constancy of the thermally induced reversible gelation upon several cycles implies that the as-cast gel was in the equilibrium state [10, 13].

As discussed before, the bridging forces are responsible of the solid-like behavior shown by these samples. However, once the shear stresses are high enough to exceed the cohesion limit (yield stress), the physical bonds break down and the product behaves as a fluid. The roughly parallel decline of G' and G'' with decreasing frequency (Fig. 3) is unusual when compared to the behavior of bulk BC [13]. This property of the gels may have implications for the network-induced memory effect [1].

The different viscoelastic behavior of the SBS-1101 film, and of its gel, can be correlated with the microstructure of the samples analyzed. Figure 6 shows TM-AFM height and phase images of SBS-1101 film in THF

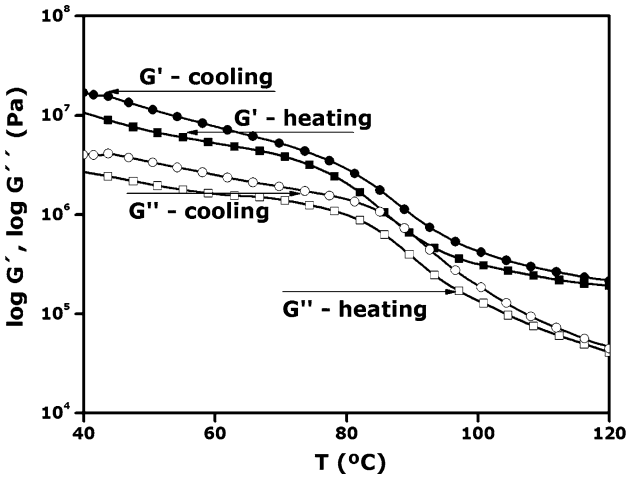

Fig. 5 Isochronal temperature ramps ($\gamma = 1\%$, $\omega = 1$ Hz, heating/cooling rate = 5 °C/min) from 40 to 120 °C for PG-SBS. G' corresponds to the fifth heating/cooling cycle. The heating ramp is characterized by *filled square*, while G'' by *unfilled square*. Whereas, for the cooling ramp G' is characterized by *filled circle*, and G'' is characterized by *unfilled circle*

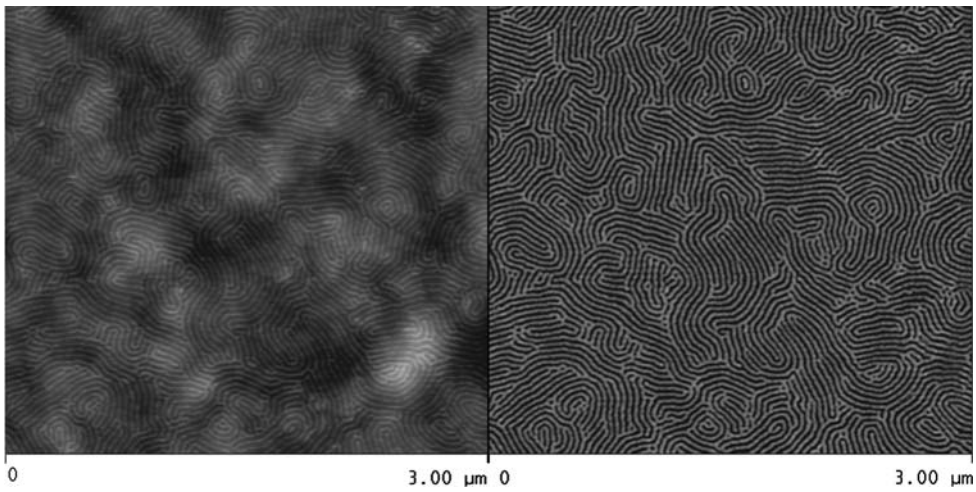

Fig. 6 TM-AFM height and phase images of SBS-1101 (in 3% THF solution)

solution. This film is not submitted to annealing treatment, and is compared to the morphology of the PG-SBS. In Fig. 6, the cylindrical nanostructure, characteristic of the not annealed films of SBS block copolymer it is well evidenced.

Figure 7 reports TM-AFM height and phase images of the physical gel obtained from SBS block copolymer and THF (3%). In particular, micellar domains with bridge conformation characteristic of gel materials can be detected. Since the bridging is an activated process [10], long-lived, isolated metastable configurations which are free of bridging are also observed.

It is interesting to note that by incorporating Ag nanoparticles in the SBS solution gelled nanocomposites of Ag/SBS can also be obtained. PG Ag SBS nanocomposites were prepared with the same technique followed in the case of pure SBS and to reach an uniform dispersion of Ag nanoparticles in the SBS matrix, DT was used as surfactant with a DT-Ag weight ratio of 1 [34, 35].

In Fig. 8, TM-AFM height and phase images of PG-Ag/SBS (1 wt% Ag with respect to SBS, 3 wt% SBS with respect to THF) are shown, while in Fig. 9 the same images are reported for a SBS-nanocomposite film with 1 wt% of Ag nanoparticles. It is possible to observe that the morphology of the two nanocomposites is remarkably different. In fact, in the solvent cast film, PS cylindrical domains are detected, while the micellar structure is once again detectable analyzing the nanostructure of the physical gel reinforced with 1 wt% of Ag.

In both cases, well-dispersed Ag nanoparticles confined in the PS block are clearly observed. Furthermore, as expected from the solubility parameters [34] calculated based on the Hoftyzer–Van Krevelen theory (Table 1), the DT-coated Ag nanoparticles show better affinity for the PS-block of the SBS block copolymer matrix (i.e., $\delta(\mathrm{DT}) = 19.2$) [34, 35].

Finally, the physical gel behavior of the PG-Ag/SBS nanocomposites has been confirmed by rheological

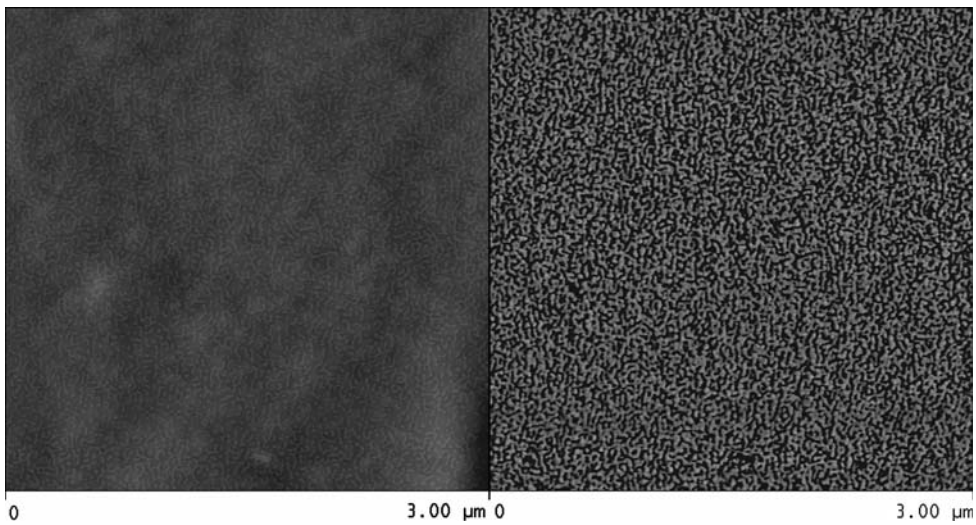

Fig. 7 TM-AFM height and phase images of PG-SBS (3 wt% in THF)

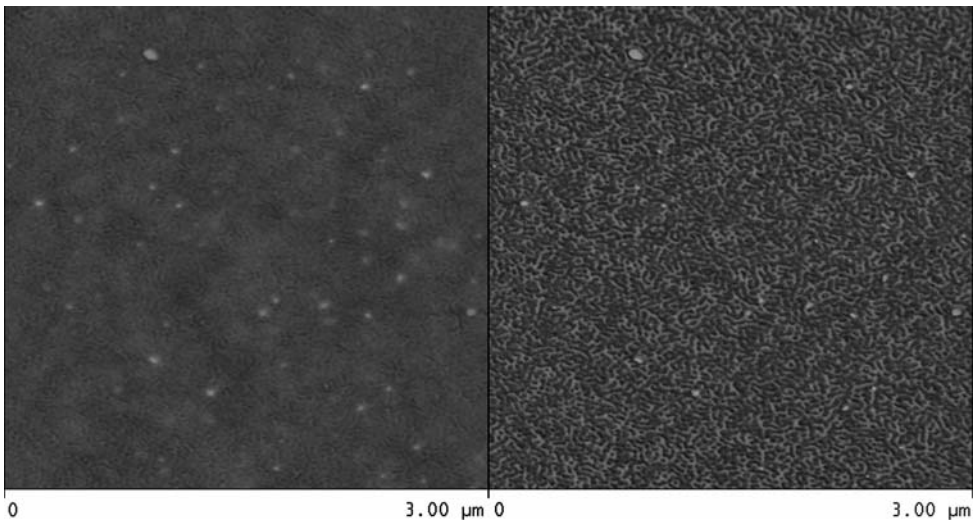

Fig. 8 TM-AFM height and phase images of PG-Ag/SBS

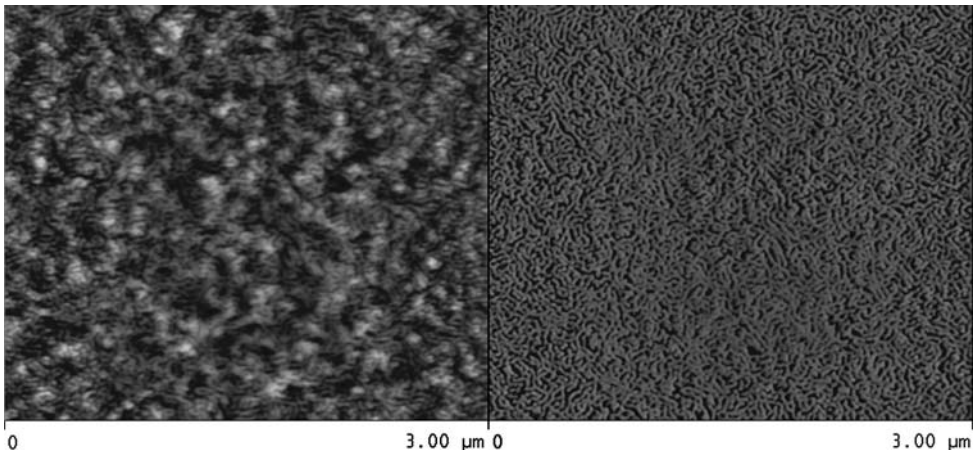

Fig. 9 TM-AFM height and phase images of Ag/SBS nanocomposite

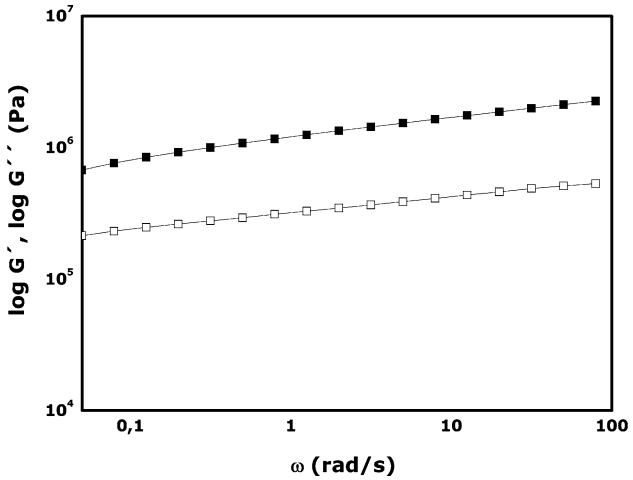

Fig. 10 Frequency dependence of G' (*filled square*) and G'' (*unfilled square*) for PG-Ag/SBS at 30 °C

analysis (Fig. 10). The gel behavior of the Ag/SBS, with 1 wt% Ag nanoparticles, is clearly evidenced by G' values higher than G'' values, almost independent of the frequency, and by the absence of the cross-over between G' and G''. It is worth to note that both G' and G'' values for the nanocomposite gel are higher than those corresponding to the PG-SBS, shown above. In particular, the higher values of G' and G'' for the nanocomposite gel indicate that the Ag nanoparticles embedded in the PS block of the SBS physical gel act as a hardening agent. Moreover, a higher increment in terms of G'' with respect to G' indicates the less elastic behavior of the nanocomposite gel with respect to that of PG-SBS. A specific study on the stability and reversibility of the PG-Ag/SBS nanocomposite will be objective of the future work.

Conclusions

The ability of SBS triblock copolymer to form physical gels in solution with a mid-block selective solvent (THF) has been analyzed in terms of viscoelastic behavior and nanostructure morphology. From a rheological point of

view, the higher value of G' with respect to G'' and the absence of a cross-over between G' and G'' and their frequency-independent behavior confirm that SBS triblock copolymers can form physical gels in mid-block-selective solvents like THF. Furthermore, AFM studies have shown a micellar nanostructure of the SBS physical gel.

Finally, the gelling capability of SBS solution of THF was kept in nanocomposites obtained dispersing Ag nanoparticles in the SBS matrix. In fact, rheological and morphological studies confirmed their gelling behavior. The rheological analysis of the PG-Ag/SBS evidenced again the absence of cross-over between G' and G'' and their frequency-independent behavior. While, from AFM studies, it was still possible to detect a micellar morphology similar to that observed for the SBS gel.

Acknowledgement This study was performed within the framework of the European Network of Excellence NANOFUN-POLY.

References

1. Whitesides GM (2005) Small 1:172
2. Yin Y, Lu Y, Gates B, Xia Y (2001) J Am Chem Soc 123:8718
3. Park C, Yoon J, Thomas EL (2003) Polymer 44:6725
4. Whitesides GM, Grzybowski B (2002) Science 295:2418
5. Nörenberg C, Castell MR (2007) Surf Sci 601:4438
6. Lazzari M, Lopez-Quintela MA (2003) Adv Mater 15:1583
7. Matsen MW, Bates FS (1997) J Polym Sci Part B Polym Phys 35:945
8. Son SU, Jang Y, Yoon KY, Kang E, Hyeon T (2004) Nano Lett 4:1147
9. Li M, Ober CK (2006) Mater Today 9:30
10. Sato T, Watanabe H, Osaki K (2000) Macromolecules 331:686
11. Nijenhuis KT (1997) Adv Polym Sci 130:1
12. Wedler W, Tang W, Winter HH, MacKnight WJ, Farris RJ (1995) Macromolecules 28:512
13. Seitz ME, Wesley RB, Faber KT, Kenneth RS (2007) Macromolecules 40:1218
14. Victorov A, Radke C, Prausnitz J (2005) J Mol Phys 103:1431
15. Miller-Chou BA, Koenig JL (2003) Macromolecules 36:4851
16. Ottone ML, Deiber JA (2005) Polymer 46:4928
17. Enlow D, Rawal A, Kanapathipillai M, Schmidt-Rohr K, Mallepragada S, Lo C-T, Thiyagarajan P, Akinc M (2007) J Mater Chem 17:1570
18. Erhardt R, Böker A, Zettl H, Kaya H, Pyckhout-Hintzen W, Krausch G, Abetz V, Müller AHE (2001) Macromolecules 34:1069
19. Watanabe H, Sato T, Osaki K, Yao M-L, Yamagishi A (1997) Macromolecules 30:5877
20. Watanabe H, Yao M-L, Sato T, Osaki K (1997) Macromolecules 30:5905
21. Kleppinger R, Van Es M, Mischenko N, Koch MHJ, Reynaers H (1998) Macromolecules 31:5805
22. Daniel C (2007) Macromol Symp 251:1
23. Vega DA, Sebastian JM, Loo Y-L, Register RA (2001) J Polym Sci Part B Polym Phys 39:2183
24. Kempe MD, Verduzco R, Scruggs NR, Kornfield JA (2006) Soft Matter 2:422
25. He Y, Boswell PG, Bühlmann P, Lodge TP (2007) J Phys Chem B 111:4645
26. Das C, Inkson NJ, Read DJ, Kelmanson MA, McLeish TCB (2006) J Rheol 50:207
27. Tung S-H, Huang Y-E, Raghavan SR (2007) Langmuir 23:372
28. Liu Z, Cattopadhyay S, Shaw MT, Hsiao BS (2004) J Polym Sci Part B Polym Phys 42:1496
29. Lionetto F, Coluccia G, D'Antona V, Maffezzoli A (2007) Rheol Acta 46:601
30. Durkee DA, Gomez ED, Ellsworth MW, Bell AT, Balsara NP (2007) Macromolecules 40:5103
31. Hamley IW, Pople JA, Gleeson AJ, Komanschekb BU, Towns-Andrews E (1998) J Appl Cryst 31:881
32. Paglicawan MA, Balasubramanian M, Kim JK (2007) Macromol Symp 249:601
33. Van Krevelen DW (1990) Properties of polymers. Elsevier, Amsterdam
34. Peponi L, Tercjak A, Torre L, Kenny JM, Mondragon I (2008) Compos Sci Technol 68:1631
35. Peponi L, Tercjak A, Torre L, Kenny JM, Mondragon I (2009) J Nanosci Nanotechnol 9:2128